TABLE OF CONTENTS

Supplementary Figures

Supplementary Methods

Supplementary Figures

Supplementary Fig. 1. Trafficking and processing of receptors. (**A**) Immunoblotting shows that NRR- and sNRR-based SynNotch receptors are processed into a noncovalent heterodimer by furin convertase. Treatment with Furin Inhibitor I (Cayman Chemical, 14965) induces the loss of cleaved N-terminal fragments (N-term, white arrowheads) and accumulation of full-length receptors (FL, black arrowhead). sNRR-based SynNotch receptors possess two myc tags N-terminal to the furin cleavage site, while NRR-based SynNotch receptors have one myc tag. Analyzed lysates were from transfected or nontransfected ("Ctrl") HEK293-FT cells (R70007, ThermoFisher). (**B**) Immunostaining of SynNotch receptors shows surface expression and NRR accessibility in HeLa cells. Receptors express a GFP-binding nanobody as the LBD, which is stained using soluble GFP (green). Wheat germ agglutinin (WGA) stains cell membranes. Control cells are nontransfected. (**C**) Similar to (**B**), except GFP is used to stain the LBD at 37 °C, rather than 4 °C, to allow receptor internalization. Subsequent fixation and anti-NRR staining reveals that surface-stained receptors are constitutively internalized and recycled from the cell surface, as evident by internalized LBD staining that does not colocalize with surface NRR staining. (**D**) Immunoblotting showed that NRR- and sNRR-based full-length recombinant human Notch1 receptors (rather than SynNotch receptors) are processed into noncovalent heterodimers, as evidenced by detection of the C-terminal fragment. Here, only sNRR receptors encode a Myc epitope; an endogenous anti-myc reactive band detected at ~100 kDa ("background") is seen in all lanes, including non-transfected control cells. Note that analyzed lysates in D were from transfected or nontransfected ("Ctrl") HEK293 cells (ATCC-CRL-1573). (**E**) Similar to (**B**), in cells expressing full-length recombinant Notch1 receptors, rather than synthetic Notch receptors. Labeling the LBD with soluble Dll4/Fc shows receptors at the cell surface. Incorporation of a sNRR domain blocks reactivity to staining with exogenous anti-NRR.
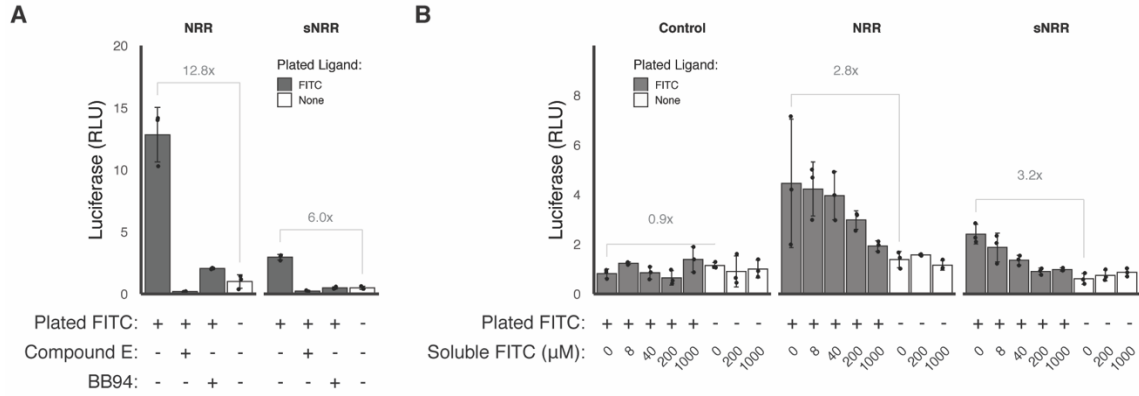
Supplementary Fig. 2. Ligand-mediated activation of receptors. Cells expressing NRR- and sNRR-based receptors containing Gal4-VP64 ICDs were cultured on control surfaces containing fibronectin only or grown in fibronectin- and FITC ligand-coated wells. Receptor activation induced the expression of a Gal4-dependent firefly luciferase reporter gene (UAS-FLuc). (**A**) Plated ligand induced luciferase reporter activity, which was reduced upon treatment with BB94 (20 µM; for metalloproteinase inhibition) or with Compound E (400 nM; a gamma secretase inhibitor). (**B**) Treatment with varying amounts of soluble fluorescein resulted in dose-dependent competitive inhibition against surface-immobilized ligands. Treatment with soluble ligands alone did not induce signaling upregulation (consistent with the notion that soluble ligands cannot offer tensile resistance to unravel the NRR or sNRR domains). Control cells express NRR-based SynNotch receptors with a tTA-based ICD, which is mismatched with respect to the implemented UAS-FLuc reporter gene. Mean ± s.d. displayed from three independent transfections (n=3). Fold change indicated on the graph.
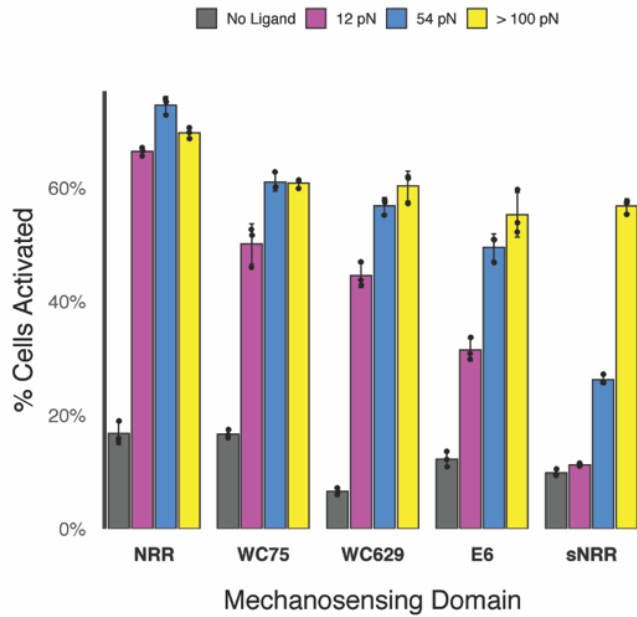
Supplementary Fig. 3. Additional NRR-scFv pairs tested on TGT's. In addition to the original scFv tested in the sNRR domain (right set of bars; gray; sequence derived from ref. 28: Wu *et al.*, *Nature* 464, 1052-1057 (2010)), three additional Notch1 NRR-binding antibodies were expressed as scFv receptor functions similar to sNRR. The tensile sensitivity of these receptors were evaluated using FITC-conjugated TGTs via transient expression in reporter HEK293-FT cells (UAS-H2B-mCherry). Mean ± s.d. from three independent transfections (n=3) displayed; quantified by flow cytometry (over 5,000 cells assessed per replicate). Quantified signaling responses are shown above; individual samples were analyzed using 1,000 cells or more.
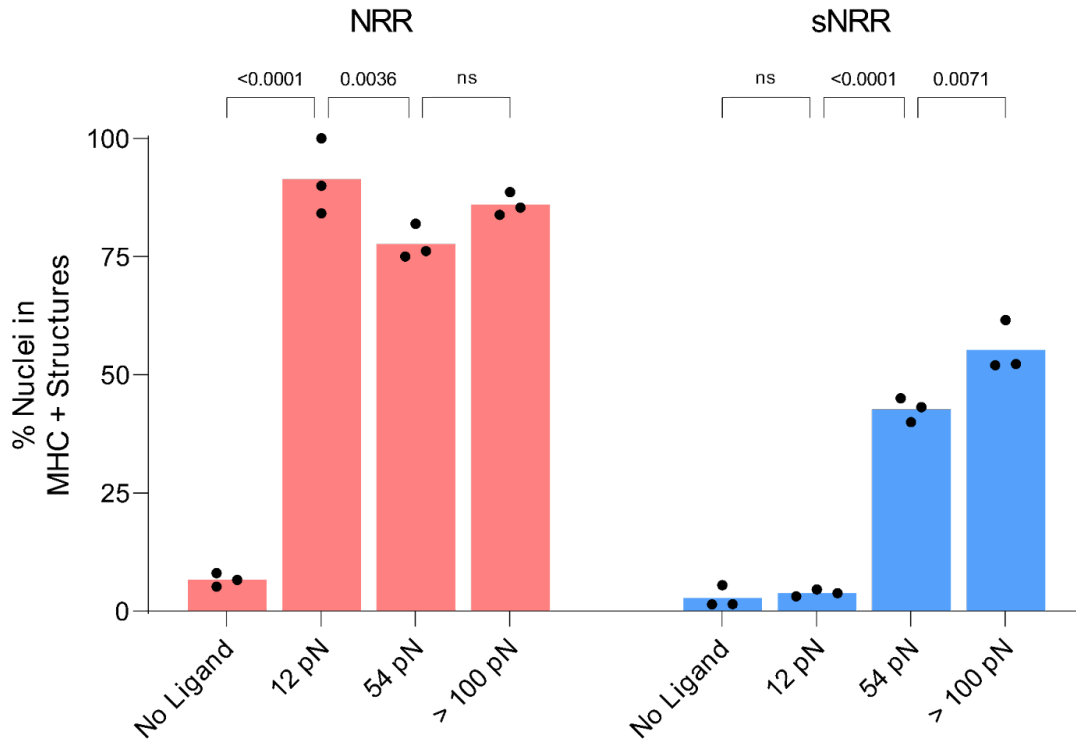
Supplementary Fig. 4. Quantification of TGT-induced myogenic differentiation. C3H10T1/2 fibroblasts expressing NRR- or sNRR-based SynNotch receptors induce p65-MyoD expression upon activation which facilitates myogenic differentiation. Extents of myogenic differentiation were quantified as percentages of DAPI-labeled nuclei localized to cellular structures with positive-costaining against Myosin Heavy Chain (MHC). Data represented as the mean from 3 immunostained fluorescence micrographs per group (n=3) using images containing 100 cells or more. Data analyzed and significance determined by 2-way ANOVA (NRR type and TGT threshold), with P-values displayed between compared conditions.
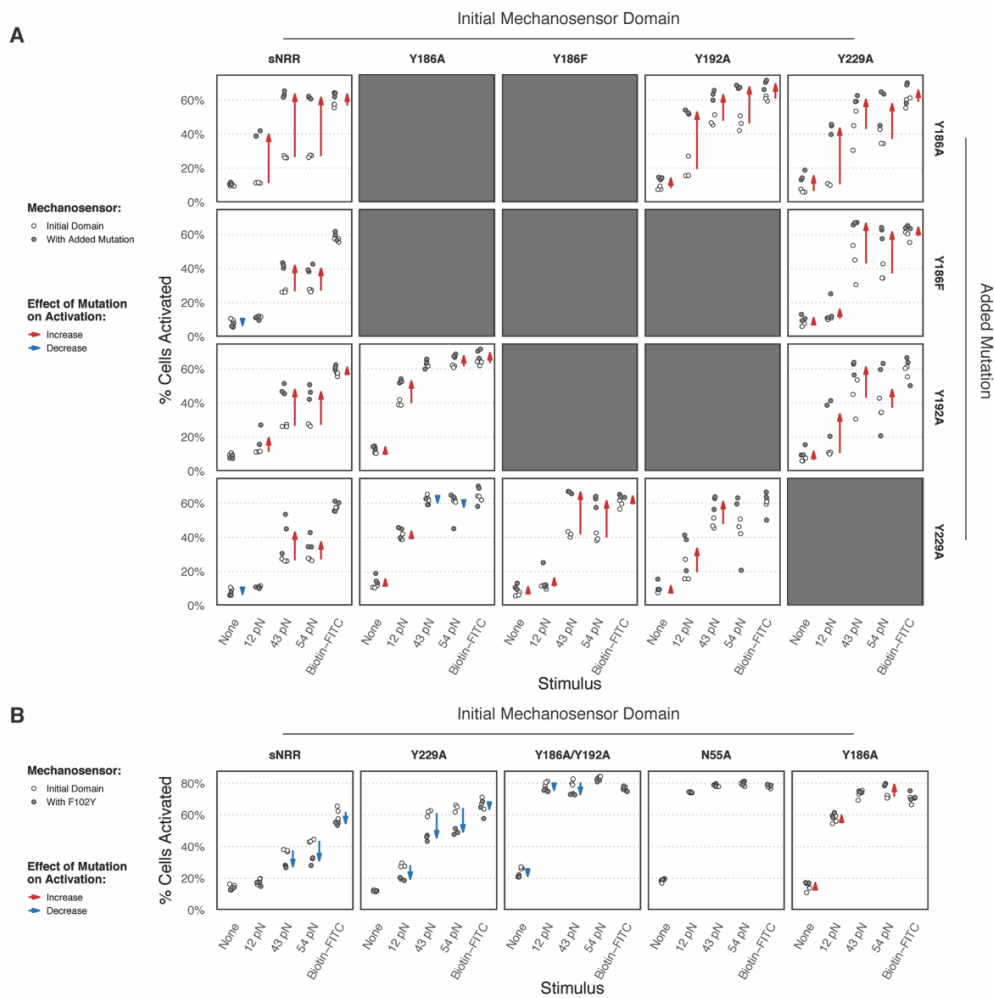
Supplementary Fig. 5. Tuning mechanical strength through double mutation or strengthening mutations. (A) An extension of the data sets presented in Figures 2D-E detailing the effects of single and double mutations on receptor mechanical strengths. Each individual plot depicts the effect of an added mutation (gray circles on plots, vertical axis of grid) on an initial mechanosensing domain (open circles on plots, horizontal axis of grid). Arrows denote the change in mean activation upon mutation, for changes of magnitude > 5%. Mutations that weaken the receptor are expected to increase activation (red), while mutations that strengthen the receptor are expected to reduce activation (blue). **(B)** Effect of the F102Y mutation, represented as in **(A)**. Addition of F102Y generally increases receptor strength, except in the case of the Y186A sNRR mutant. Note that the amino acid position corresponding to Y186A is positioned adjacent to and comes into contact with F102 in three-dimensional space. **(C)** Modeled mutagenesis depicting F102Y. F102Y adds a hydroxyl group at the *para*-position. Rotamer modeling predicts this group would sterically fit at the binding interface and would be solvent-exposed (model based on PDB 3L95).
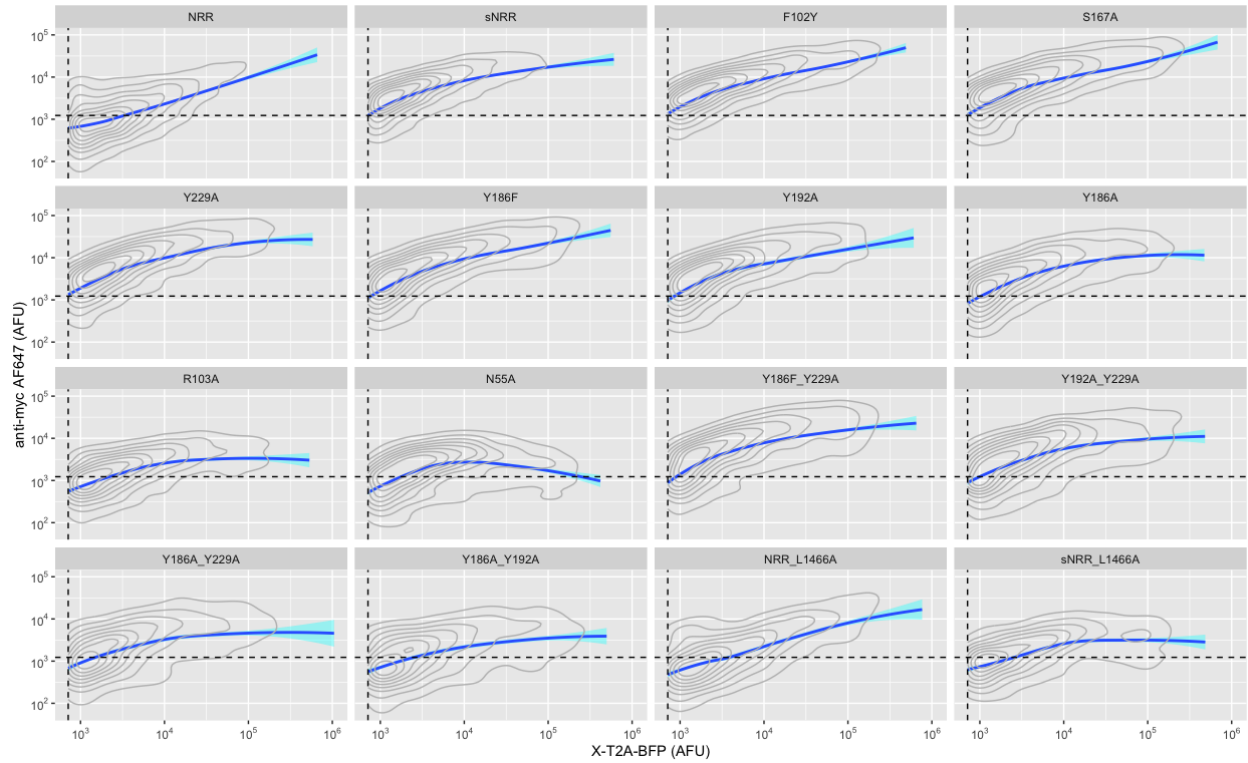
Supplementary Fig. 6. Comparison of mechanoreceptors surface presentation levels. Sixteen individual sNRR domains exhibiting differing mechanical properties were expressed as T2A-BFP fusion constructs via transient transfection in HEK293-FT cells. The surface expression levels of each construct were determined via live cell staining with anti-myc-AlexaFluor647 antibody. Surface staining intensities were then compared against BFP emissions using flow cytometry. Contour plots of total BFP+ cells from three independent transfections shown with 10 contour bins (n=3). Dark blue line is a LOESS smooth curve, with cyan denoting 95% confidence level. BFP and AF647 thresholds (dashed horizontal and vertical lines, respectively) were calculated from non-transfected and unstained HEK293-FT cells.

ICD: Gal4-VP64   Gal4-VP64-p65   Gal4-VP64-p65-RTA

Legend: sNRR, Y49F, Y49A, NRR

Reporter Expression (AFU)
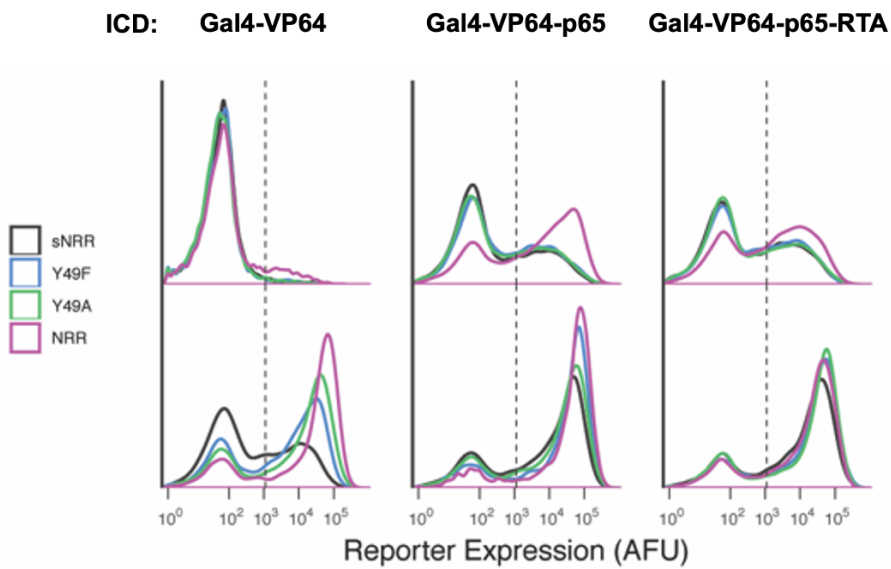
Supplementary Fig. 7. Ligand independent activation in receptors. Receptors containing the indicated ICDs were stably integrated into HEK293-FT cells. ICDs of high transcriptional potency, including VP64-p65 and VP64-p65-RTA, resulted in elevated levels of ligand-independent transcriptional activity due to the strong gene expression mediated by ligand-independently cleaved ICDs. sNRR-based receptors exhibited reduced ligand-independent activity (LIA) compared to those containing NRR.
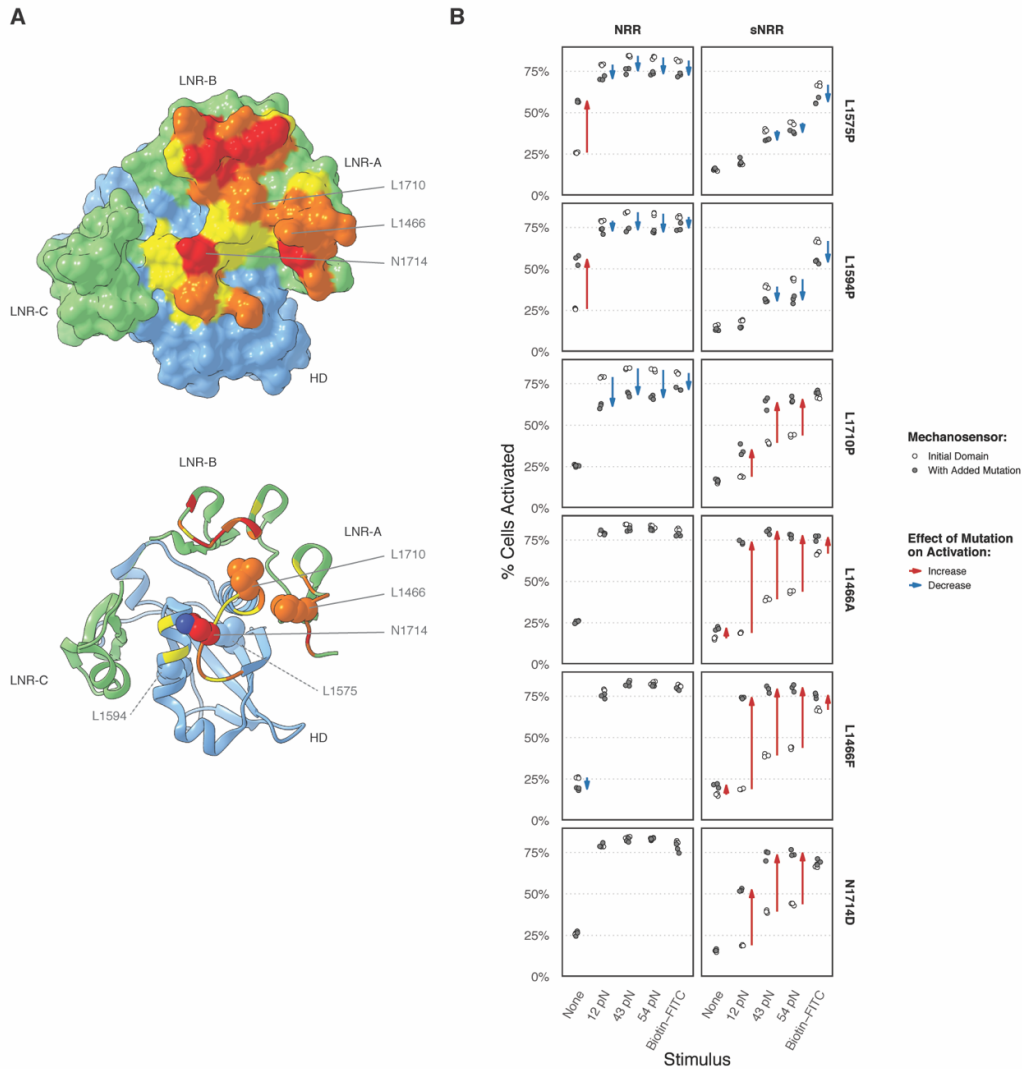
Supplementary Fig. 8. Effect of NRR mutations on sNRR tensile strength. (**A**) Surface view (top) of the Notch1 NRR, with anti-Notch1 Fab binding interface colored in yellow/orange/red, as in main Figure 2B. Mutated residues are denoted. Ribbon view (bottom) reveals all mutated residues in sphere representation, including those internal to the NRR distal to the binding interface (L1575 and L1594). L1575P and L1594P are cancerous mutations, known to destabilize the NRR and distal to the scFv-binding site. L1710P is a cancerous NRR mutation within the scFv-binding interface (PDB 3L95). (**B**) The effect of mutations on receptor strength. Each individual plot depicts the effect of an added mutation (gray circles on plots, vertical axis of grid) on an NRR or sNRR mechanosensing domain (open circles on plots, horizontal axis of grid). Arrows denote the change in mean activation upon mutation, for changes of magnitude > 5%. Mutations that weaken the receptor are expected to increase activation (red), while mutations that strengthen the receptor are expected to reduce activation (blue). L1575P and L1594P destabilize the NRR's autoinhibited conformation, causing leaky activation in the absence of tension, while not greatly affecting sNRR domains. L1466A, L1466F, and N1714D, which reside at the scFv:NRR binding interface, but away from the LNR stabilizing interface in WT NRR, destabilize sNRR domains without affecting NRR activation. L1710P exists at the overlap of NRR's natural stabilizing interface and sNRR's engineered scFv interface, and in turn it impacts signaling of both receptors.
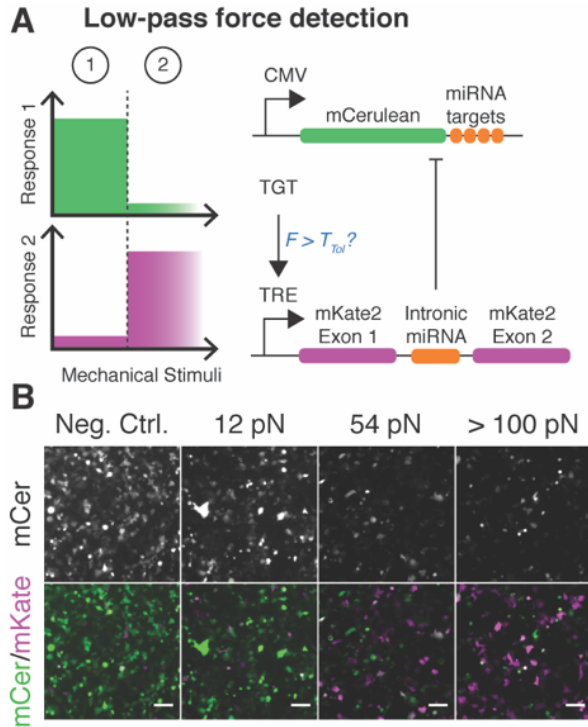
Supplementary Fig. 9. Low pass filtering in mechanogenetic circuits. (**A**) Anticipated signaling responses and circuit diagram showing a constitutively transcribed mCerulean gene, the mRNA transcript of which is targeted for miRNA-mediated degradation via fusion with 3' miRNA targeting sequences. Expression of a corresponding FF4 miR from an intronic TRE-regulated mKate2 construct results in degradation of the mCerulean target mRNAs. Receptors with a tTA ICD induce TRE-driven mKate2 mRNA simultaneously with FF4-miRNA via intronic splicing. TRE-promoter activation thus results in increased mKate2 emission, alongside reduced mCerulean expression, due to miRNA targeting of the mCerulean gene. (**B**) Fluorescence images of HEK293FT cells expressing the low-pass circuit components and stimulated with TGTs. mCerulean expression is only detected only in response to low T_{tol} TGTs; high T_{tol} TGTs induce mKate2 expression concurrently with reduction of mCerulean. Scale bars are 100 μm.
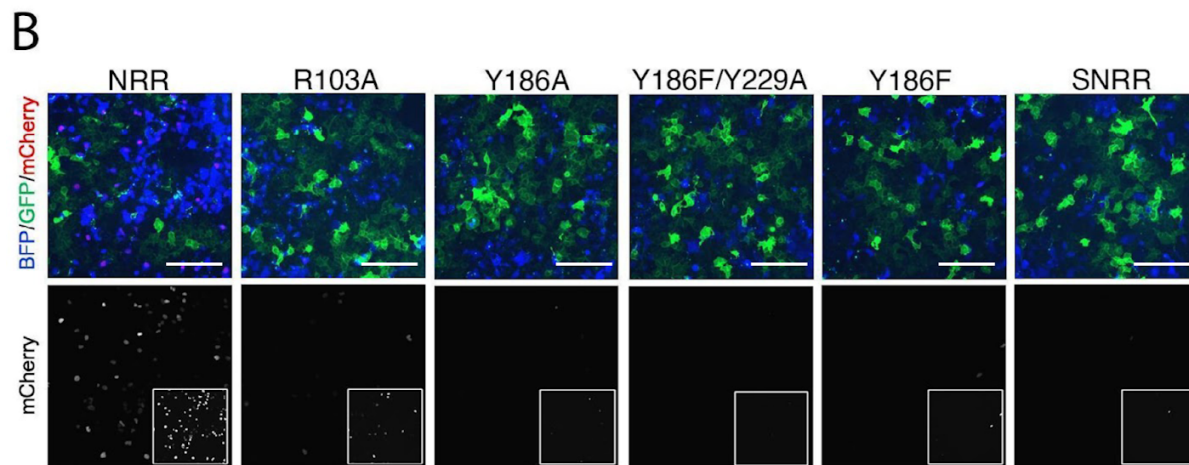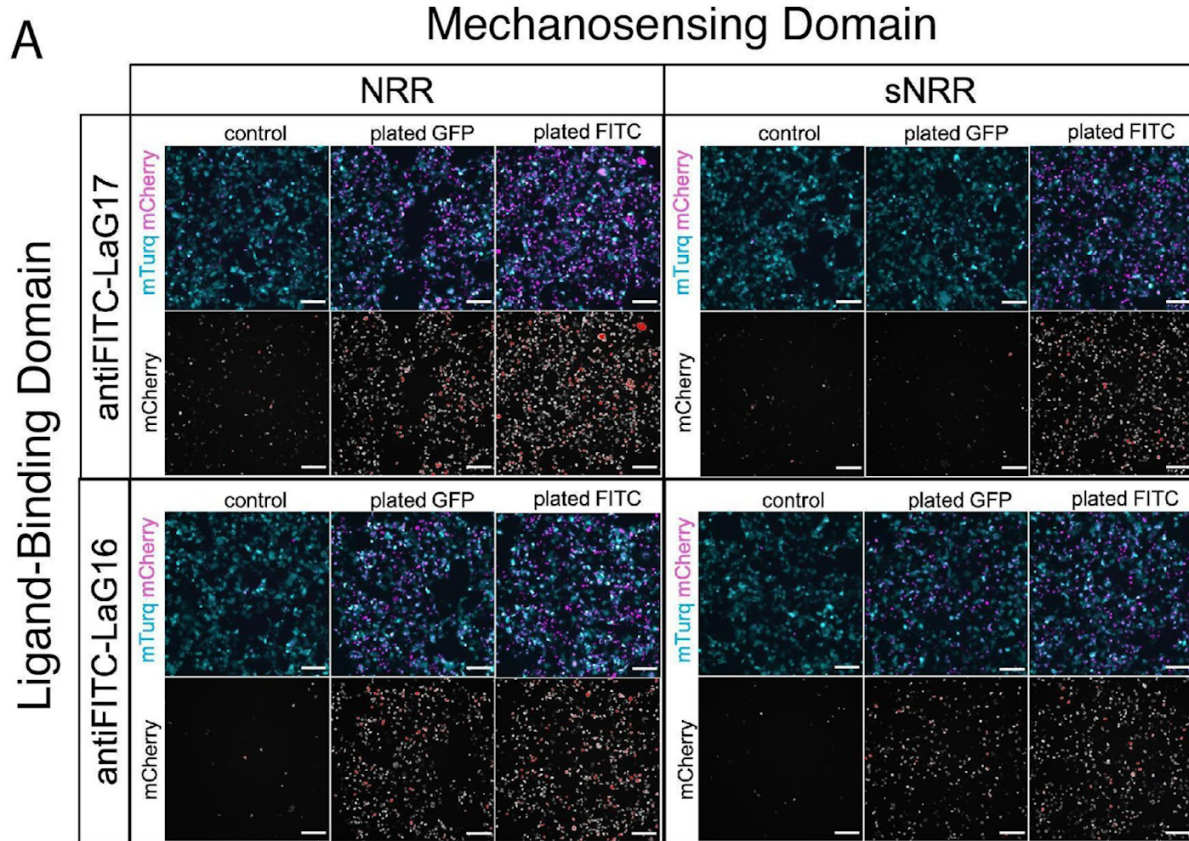
Supplementary Fig. 10. LaG16-mediated recognition of GFP facilitates sNRR activation. (**A**) Cells expressing LaG16-sNRR exhibit signaling responses when grown on surfaces containing neutravidin-immobilized mono-biotinylated-GFP, whereas cells-expressing LaG17-sNRR are refractory against the immobilized ligand. Images represent reporter (H2B-mCherry; red) expression in transiently transfected HEK293-FT reporter cells (UAS-H2B-mCherry). A plasmid encoding constitutively expressed by mTurquoise2 was utilized as a transfection marker. (**B**) Transduced reporter cells expressing receptors expressing LaG17-based ECDs displayed reduced, or non-detectable signaling activities when grown in coculture with HEK293-FT GFP-DLL1 sender cells. These results contrast with the *trans*-cellular action of receivers expressing LaG16-based receptors (displayed in main Fig. 4B). We note that these data suggest a restriction in the propagation of tension across single LaG17-GFP bonds. Scale bars in A and B are 200 µm.
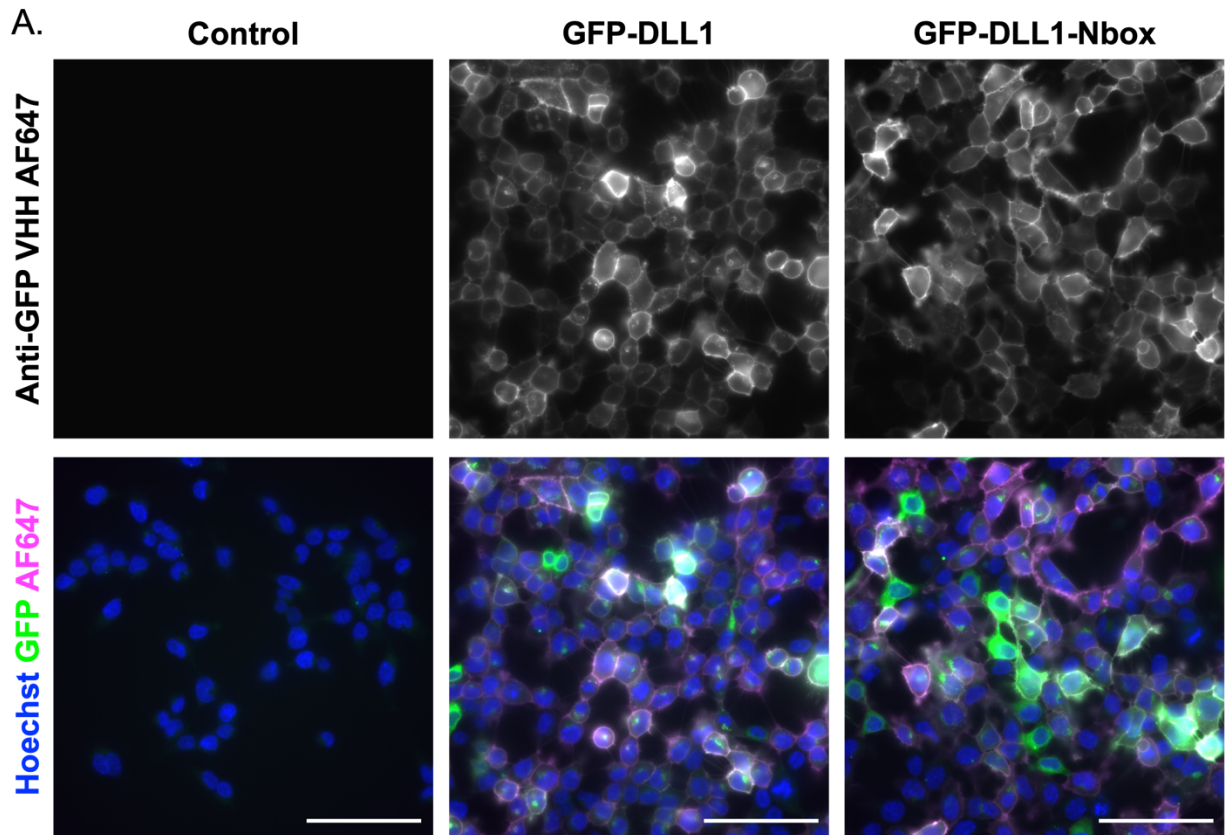
Supplementary Fig. 11. Cell surface detection of GFP-based ligands. (**A**) Transduced sender HEK293-FT cells bearing TRE-regulated GFP-TMD-DLL1 and GFP-TMD-DLL1-Nbox constructs were treated with 100 ng/mL doxycycline for 24 hours prior to live cell staining with an anti-GFP VHH coupled to AlexaFluor647 ("GFP-Booster AlexaFluor647," AF647; grayscale in top row; magenta in bottom row). Non-transduced HEK293-FT cells were utilized as a control (right-side images); cells were counterstained with Hoechst 33342 to highlight nuclei (blue); direct GFP fluorescence detection is shown in green. Images were collected under live conditions in PBS, following washing out of unbound VHH (see Materials and Methods). Scale bars are 100 μm.
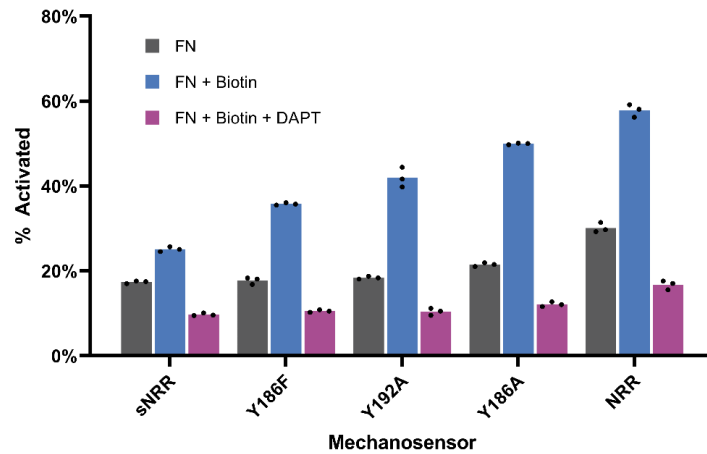
Supplementary Fig. 12. Tensile stability of anti-biotin:biotin bonds are sufficient for strengthened receptor activation. (**A**) The ability of anti-biotin:biotin bonds in mediating sNRR activation was determined by transient transfection of HEK293-FT reporter cells (UAS-H2B-mCherry) with receptors constructs containing anti-biotin-scFv based ECDs. Cells were grown in the presence of wells coated with biotinylated BSA, or in control wells containing coated only with fibronectin. Signaling responses were quantified via flow cytometry, with comparison of cells on control surfaces (gray bars), or on biotin-coated surfaces (blue bars), or in the presence of biotinylated surfaces with gamma secretase inhibition (DAPT at 10 μM). The results confirm the ability of scFv-biotin bonds to withstand the tensile forces required for sNRR activation. Biological triplicate, 2-way ANOVA statistical test show f < 0.001 for each between each condition.

A.

B.

C.

HEK 293   0   2 pM   20 pM   200 pM   2 nM   20 nM   200 nM   2 uM   20 uM   20 nM + DAPT

— 50 kDa
— 40 kDa
— 30 kDa

H2B-mCherry (anti-RFP)

— 30 kDa

GAPDH
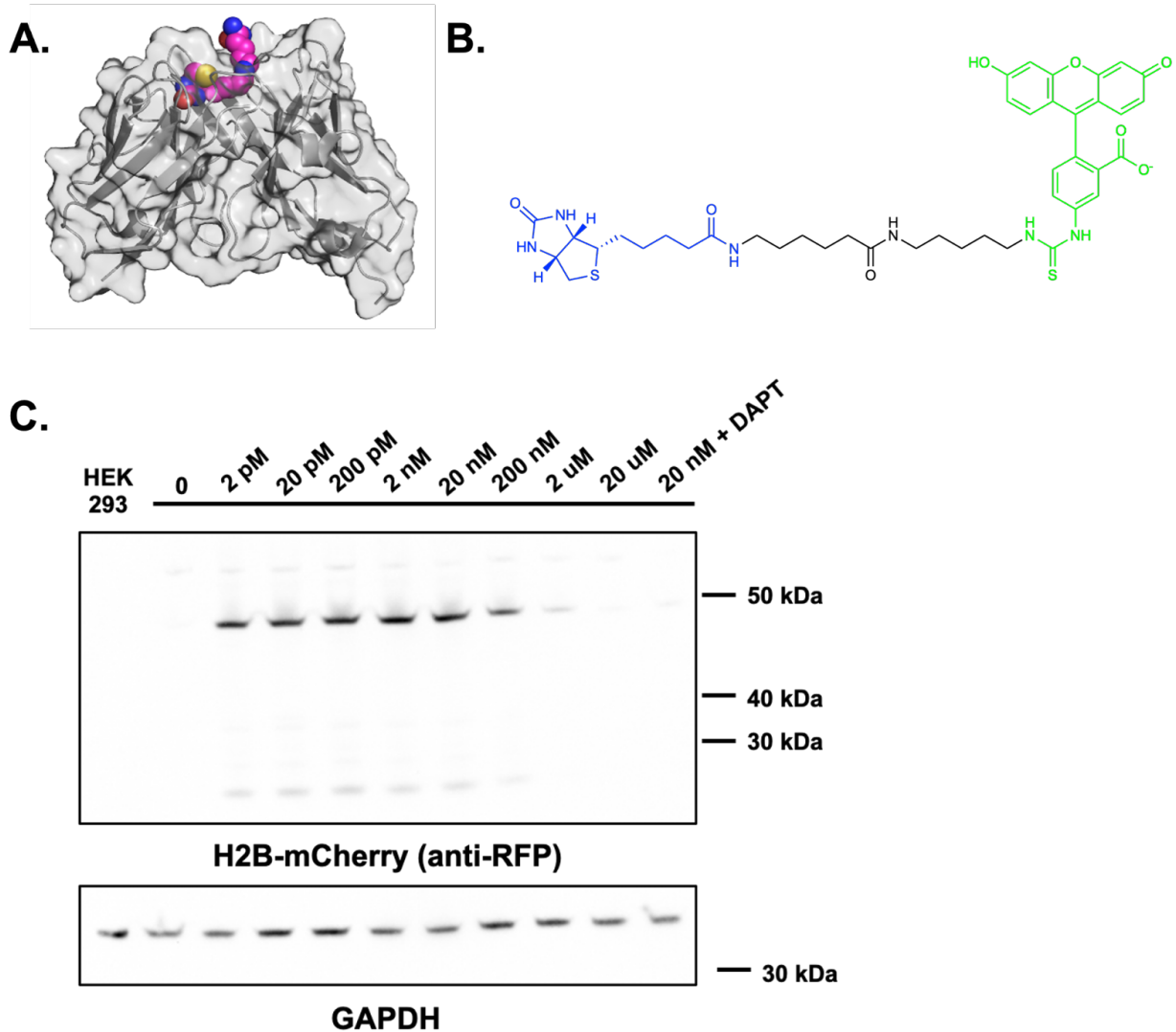
Supplementary Fig. 13. Inducible *trans*-cellular coupling using a bifunctional small molecule based on biotin-FITC. (**A**) Structure of the biotinamide-binding antibody fragment as an scFv with biotinamide shown as spheres (based on PDB: 4S1D). (**B**) Chemical structure of the biotin-linked fluorescein compound used (biotin-FITC; 25574, Cayman Chemical, CAS Number 134759-22-1). Biotinamide and FITC moieties are shown in blue and green, respectively. (**C**) Western blow of lysates from sender-receiver cocultures. Reporter HEK293-FT (UAS-H2B-mCherry) cells stably expressing a CMV-driven anti-FITC-NRR-SynNotch-Gal4-VP64-mTurq2 receptor were cultured in combination with stable HEK293-FT senders expressing anti-biotin-TMD-DLL1 ligand. Cells were treated with the indicated concentrations of biotin-FITC, with 20 nM biotin-FITC in combination with 10 µM DAPT or left untreated. Control lysate was derived from non-transfected HEK293-FT cells. Biotin-FITC induced H2B-mCherry protein was probed using a polyclonal anti-RFP antibody (see Materials and Methods). Cells were mixed at 1:1 a sender-receiver ratio and distributed in fibronectin coated 96 well plate microwells. Biotin-FITC was added following adherence (~4 hours later) under conditions of ~95% confluence. Cell lysis was carried out after 24 hours of drug treatment. Note: the lower mass anti-RFP reactive band observed in (**C**) represents a cleaved mCherry fragment formed due to intramolecular protein cleavage during lysate denaturation by heating.
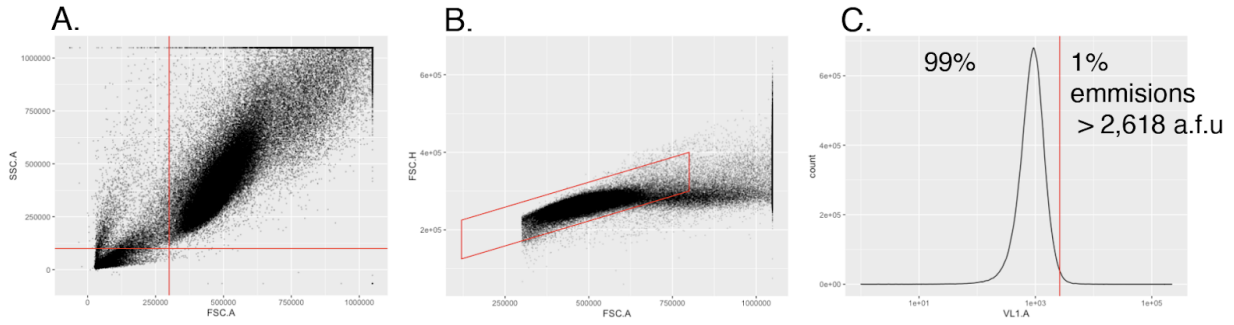
Supplementary Fig. 14. Flow cytometry gating scheme. (**A**) Live cells were gated using SSC-A and FSC-A thresholds, defined by the indicated red lines. (**B**) Singlets were isolated using a polygon gate based on FSC-H vs FSC-A as indicated by the red outline. (**C**) Fluorescence gate for isolating receptor expressing cells (in this example T2A-BFP+) was defined as the 99% percentile of control non-transduced cells, analyzed under identical excitation and detection parameters. Same was done for defining reporter activation thresholds.
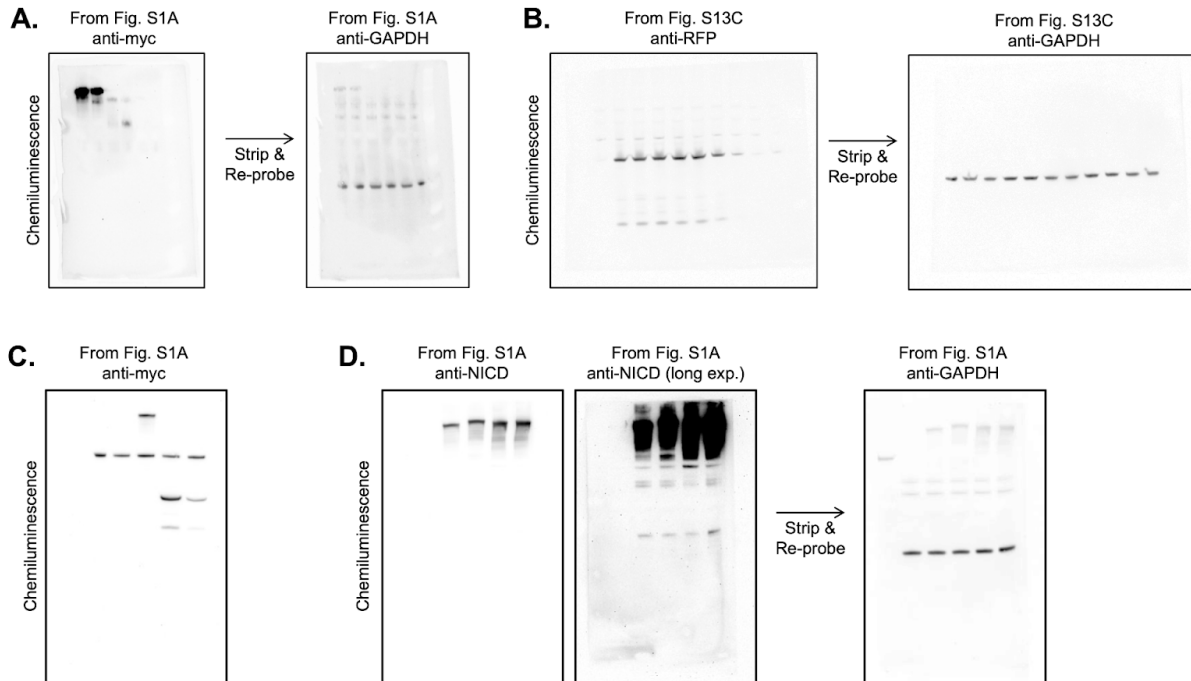
Supplementary Fig. 15. Full scans of immunoblots. Full scans of immunoblots that are presented in the figures. The blot images in A and B were captured on a ThermoFisher iBright imaging system. Those in C and D were captured using a BioRad ChemiDoc imager. For the blots in panels C and D, only the first three rightmost sample-containing lanes are presented in the figures (from left to right: control, NRR, sNRR); the remaining 2 leftmost lanes represent samples/constructs that are not related to nor reported in the present paper. All blots contained PageRuler Prestained Protein Ladder (26616, ThermoScientific); for the blots in panels A and B the molecular weight ruler was loaded into a lane on right following the sample containing lanes, for the blots in C and D the ladder was loaded into a lane to the left of the sample containing lanes. For the blot in C a background (non-myc) endogenous protein band (of ~100 kDa mass) served as a loading control; note that the lysates analyzed in panels C and D derive from transfected or non-transfected (control) HEK293 cells, whereas the lysates analyzed in A and B derive from transfected or nontransfected HEK293-FT cells.

Supplementary Methods
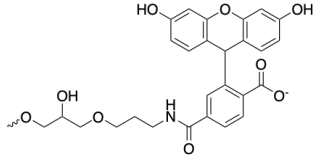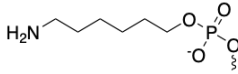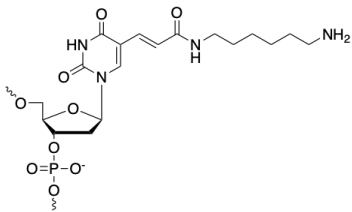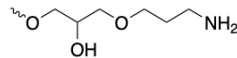
Antibodies and Labeling Proteins

Commercial antibodies and labeling proteins were used at the indicated dilutions:

Antibody or Labeling Protein	Dilution	Product Number and Supplier
Mouse anti-myc-AlexaFluor647	1:200	sc-40 AF647, Santa Cruz Biotechnology
Mouse anti-myc-Alexa Fluor488	1:200	MA1-980-AF488, ThermoFisher
Mouse anti-myc	1:200	AHO0062 (Clone 9E10), ThermoFisher
Mouse anti-myosin heavy-chain	1:100	MAB4470 (Clone MF20), R&D Systems
Mouse anti-NRR E6	1:1,000	Ab00175-1.1, Absolute Antibody
Mouse anti-Notch1 E4 (C-term)	1:500	sc-373944, Santa Cruz Biotechnology
Rabbit anti-RFP	1:1000	600-401-379, Rockland Immunochem.
GFP-Booster AlexaFluor647	1:500	gb2AF647-50, ChromoTek/Proteintech
Mouse anti-GAPDH	1:3,000	MA5-15738, ThermoFisher
Direct-Blot HRP anti-GAPDH	1:4,000	607904, BioLegend
Anti-mouse-HRP	1:3,000	7076, Cell Signaling Technology
Anti-rabbit-HRP	1:3,000	1721019, Bio-Rad
Goat anti-mouse-AlexaFluor488	1:2,000	A-11001, ThermoFisher
Rabbit anti-mouse-AlexaFluor647	1:1,000	A-21239, ThermoFisher
Goat anti-human-AlexaFluor647	1:1,000	A-21445, ThermoFisher
Dll4Fc (human Fc)	5 µg/mL	A42511, ThermoFisher
WGA-AlexaFluor647	4 µg/mL	W32466, ThermoFisher

In-house purified proteins were prepared as described in subsequent sections and used at the concentrations indicated below:

Purified Protein	Concentration
Anti-Notch1-NRR-scFv-Fc	1 µg/mL for cell labeling solutions
eGFP	20 µg/mL for cell labeling solutions
biotinylated-eGFP	100 nM for ligand immobilization solutions

Chemical Structures for Oligonucleotide Modifications Used for TGT Synthesis

IDT code	Name	Structure
36-FAM	3' 6-FAM (6-fluorescein)	
5AmMC6	5' Amino Modifier C6	
iAmMC6T	Int Amino Modifier C6 dT	
3AmMO	3' Amino Modifier	

sNRR Construct Design and Numbering Convention for Mutant Domains

Mutations were introduced within the sNRR domain at positions residing within scFv or NRR regions. Amino acid positions within the scFv region were numbered order of insertion from 1 to 244. For the NRR, positions were identified based on their full-length Notch-1 numbering number designations. These conventions are depicted in the sNRR-SynNotch diagram below.
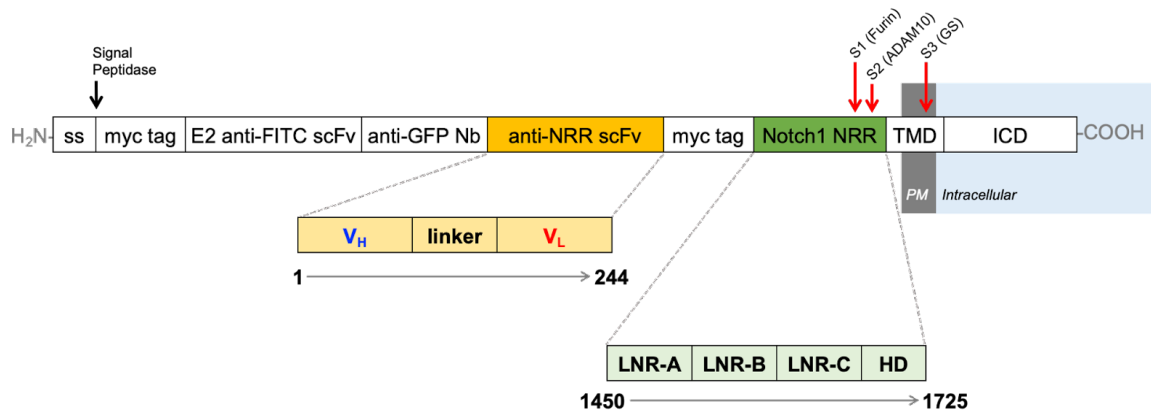
Note that the second myc tag between the anti-NRR scFv and NRR appears only in sNRR; NRR-SynNotch sequences contain only 1 myc tag, positioned N-terminally to the anti-FITC domain. Abbreviation and designations in the diagram above are defined as follows: **ss** - signal sequence peptide from CD8a, V_H - heavy chain variable region, V_L - light chain variable region, **Nb** - Nanobody (the LaG16 Nb was used for receptor *trans*-activation), **HD** - heterodimerization domain.

Anti-Notch1 NRR scFv sequence used in sNRR generation

The scFv sequence for the anti-Notch1 NRR antibody fragment is provided below with the associated numbering used in the designation of mutated scFv positions. Blue letters designate V_H residues, black indicates linker residues, red correspond to V_L residues. Mutated positions are bolded and highlighted in yellow.

```
1         10        20        30        40        50
|         |         |         |         |         |
EVQLVESGGGLVQPGGSLRLSCAASGFTFSSYWIHWVRQAPGKGLEWVAR

51        60        70        80        90        100
|         |         |         |         |         |
INPPNRSNQYADSVKGRFTISADTSKNTAYLQMNSLRAEDTAVYYCARGS

101       110       120       130       140       150
|         |         |         |         |         |
GFRWVMDYWGQGTLVTVSSGGSSRSSSSGGGGSGGGGDIQMTQSPSSLSA

151       160       170       180       190       200
|         |         |         |         |         |
SVGDRVTITCRASQDVSTAVAWYQQKPGKAPKLLIYSASFLYSGVPSRFS

201       210       220       230       240
|         |         |         |         |
GSGSGTDFTLTISSLQPEDFATYYCQQFYTTPSTFGQGTKVEIK
```

The scFv sequence above was designed based on sequence information for anti-Notch1 NRR fragment antigen-binding (Fab) reported by Wu *et al. Nature* 464, 1052–1057 (2010). Additional anti-Notch1 NRR utilized in designing the constructs analyzed in Figure S3 were originally described as follows: the anti-Notch1 NRR "E6" antibody is described in Falk et al. *Methods* 58.1, 69-78 (2012); the anti-Notch1 NRR antibodies "WC75" and "WC629" are described in Aste-Amézaga *et al. PloS One* 5.2, e9094 (2010).

DNA Sequence for the Parental sNRR domain

Blue letters designate DNA encoding anti-NRR V_H residues, red letters correspond to anti-NRR V_L residues, and letters in green highlighting encode a myc-epitope/linker. The region encoding the 'SynNotch core' component (mouse Notch-1 NRR with TMD) is shown with capitalized letters in orange text.

```
gaagtacagctggtggagtccggcggtggcctcgtgcaacccggagggtccttgaggctgtcctgtgcagccagcggt
ttcacgttcagcagctactggattcactgggtgaggcaagctccgggcaagggcctggagtggggttgcgaggataaac
cccccaacaggtccaaccagtacgccgatagcgtgaagggtcggttcaccatcagcgccgacactagcaagaacacg
gcctacctgcagatgaactctctgagggccgaggacacagcggtgtactattgcgccagggctcagggtttcgatgg
gtcatggattactggggccaaggcacccctggttaccgtttctagcggcggatctagcaggagctcatcatccgggggt
ggcgggagcggaggtggtgggatattcagatgacgcaatctccgtcctccctcagcgcaagcgtgggcgacagggtg
accattacttgtcgcgcctctcaggatgtgagcactgctgtggcctggtatcaacaaaaacccggcaaagcccccaaa
ctgctgatctactctgccagctttctgtactcaggcgtgcccagcaggttttccggctccggcagcggcaccgacttc
acccttaccattagcagcctgcagcccgaggattttgcaacctactactgccaacagttctacaccactcccagcact
ttcggccagggcacgaaggttgagatcaaggggggaggaagtgagcaaaagctgatttccgaggaggacctttggaggg
ggctccATCCTGGACTACAGCTTCACAGGTGGCGCTGGGCGCGACATTCCCCCACCGCAGATTGAGGAGGCCTGTGAG
CTGCCTGAGTGCCAGGTGGATGCAGGCAATAAGGTCTGCAACCTGCAGTGTAATAATCACGCATGTGGCTGGGATGGT
GGCGACTGCTCCCTCAACTTCAATGACCCCTGGAAGAACTGCACGCAGTCTCTACAGTGCTGGAAGTATTTTAGCGAC
GGCCACTGTGACAGCCAGTGCAACTCGGCCGGCTGCCTCTTTGATGGCTTCGACTGCCAGCTCACCGAGGGACAGTGC
AACCCCCTGTATGACCAGTACTGCAAGGACCACTTCAGTGATGGCCACTGCGACCAGGGCTGTAACAGTGCCGAATGT
GAGTGGGATGGCCTAGACTGTGCTGAGCATGTACCCGAGCGGCTGGCAGCCGGCACCCTGGTGCTGGTGGTGCTGCTT
CCACCCGACCAGCTACGGAACAACTCCTTCCACTTTCTGCGGGAGCTCAGCCACGTGCTGCACACCAACGTGGTCTTC
AAGCGTGATGCGCAAGGCCAGCAGATGATCTTCCCGTACTATGGCCACGAGGAAGAGCTGCGCAAGCACCCAATCAAG
CGCTCTACAGTGGGTTGGGCCACCTCTTCACTGCTTCCTGGTACCAGTGGTGGGCGCCAGCGCAGGGAGCTGGACCCC
ATGGACATCCGTGGCTCCATTGTCTACCTGGAGATCGACAACCGGCAATGTGTGCAGTCATCCTCGCAGTGCTTCCAG
AGTGCCACCGATGTGGCTGCCTTCCTAGGTGCTCTTGCGTCACTTGGCAGCCTCAATATTCCTTACAAGATTGAGGCC
GTGAAGAGTGAGCCGGTGGAGCCTCCGCTGCCCTCGCAGCTGCACCTCATGTACGTGGCAGCGGCCGCCTTCGTGCTC
CTGTTCTTTGTGGGCTGTGGGGTGCTGCTGTCCCGCAAGCGCCGGCGG
```

AddGene Depositions of DNA constructs

Plasmid DNA and full sequence information for the following constructs have been deposited to AddGene under the listed deposition numbers.

Deposited Plasmid	Plasmid #	Notes
LV UAS-T2A-DsRed-Express2-PGK-Puro	190801	*5xUAS/Gal4 reporter*
LV anti-FITC-LaG16-NRR-T2A-BFP	194929	*EF1A promoter with IRES-Hygro. NRR*
LV anti-FITC-LaG16-sNRR-T2A-BFP	194930	*Parental sNRR*
LV anti-FITC-LaG16-Y186F-T2A-BFP	194931	
LV anti-FITC-LaG16-Y186A-T2A-BFP	194932	
LV anti-FITC-LaG16-Y192A-T2A-BFP	194933	
LV anti-FITC-LaG16-Y186F/Y229A-T2A-BFP	194934	*2x mutant sNRR*
LV anti-FITC-LaG16-R103A-T2A-BFP	194935	
LV TRE-GFP-TMD(PDGFR)-DLL1	194936	*Doxycycline-inducible with IRES-Puro*
LV TRE-GFP-TMD(PDGFR)-DLL1-Nbox	194937	*Contains ablated Nbox motif within the DLL1 ICD (triple Ala substitution: IKNTNKK to IAAANKK)*
pBAD-6xHis-AviTag-ALFAtag-eGFP	195854	*Express in AVB101 E. coli for efficient biotinylation*